

## Article

# Shifts in Product Distribution in Microwave Plasma Methane Pyrolysis Due to Hydrogen and Nitrogen Addition

Mateusz Wnukowski <sup>1,\*</sup> , Julia Gerber <sup>2</sup> and Karolina Mróz <sup>1</sup>

<sup>1</sup> Faculty of Mechanical and Power Engineering, Wrocław University of Science and Technology, 27 Wybrzeże St. Wyspińskiego, 50-370 Wrocław, Poland

<sup>2</sup> Empa, Swiss Federal Laboratories for Materials Science and Technology, Automotive Powertrain Technologies Laboratory, 8600 Dübendorf, Switzerland

\* Correspondence: mateusz.wnukowski@pwr.edu.pl

**Abstract:** Methane pyrolysis can produce many valuable products besides hydrogen, e.g., C<sub>2</sub> compounds or carbon black. In the conditions provided by microwave plasma, the distribution of these products might be shifted by the addition of hydrogen and nitrogen. In this work, different ratios of H<sub>2</sub>:CH<sub>4</sub>, ranging from 0:1 to 4:1, were tested. The most unambiguous and promising result was obtained for the highest H<sub>2</sub>:CH<sub>4</sub> ratio. For this ratio, a significant improvement in methane conversion rate was observed (from 72% to 95%) along with the increase in C<sub>2</sub>H<sub>2</sub> and C<sub>2</sub>H<sub>4</sub> yield and selectivity. The results support the hypothesis that the H radicals present in the plasma are responsible for improving methane conversion, while the presence of molecular hydrogen shifts the product distribution towards C<sub>2</sub> compounds. Based on the carbon balance, the increase in the output of C<sub>2</sub> compounds was obtained at the cost of solid carbon. At the same time, the addition of hydrogen resulted in the formation of bigger carbon particles. Finally, with the addition of both nitrogen and hydrogen, the formation of carbon was completely inhibited. Hydrogen cyanide was the main product formed instead of soot and some of the acetylene.



**Citation:** Wnukowski, M.; Gerber, J.; Mróz, K. Shifts in Product Distribution in Microwave Plasma Methane Pyrolysis Due to Hydrogen and Nitrogen Addition. *Methane* **2022**, *1*, 286–299. <https://doi.org/10.3390/methane1040022>

Academic Editor: Patrick Da Costa

Received: 1 October 2022

Accepted: 7 November 2022

Published: 15 November 2022

**Publisher's Note:** MDPI stays neutral with regard to jurisdictional claims in published maps and institutional affiliations.



**Copyright:** © 2022 by the authors. Licensee MDPI, Basel, Switzerland. This article is an open access article distributed under the terms and conditions of the Creative Commons Attribution (CC BY) license (<https://creativecommons.org/licenses/by/4.0/>).

**Keywords:** methane coupling; C<sub>2</sub> compounds; hydrogen cyanide

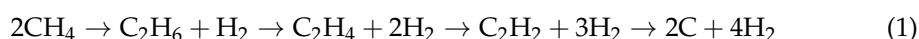
## 1. Introduction

Methane pyrolysis is often considered a possible process for CO<sub>2</sub>-free hydrogen production [1,2]. However, this process would require a sustainable source of heat necessary for methane decomposition. One of the solutions would be plasma that can be sourced with renewable energy (i.e., wind or solar). Moreover, plasma technologies usually provide an instant on/off procedure, with no need for heating up or cooling down the reactor, thus fitting well with time-variable energy sources.

While methane pyrolysis for hydrogen production has strong competition in water electrolysis, and may be considered a supplementary solution, the process is producing other valuable components, i.e., C<sub>2</sub> compounds (acetylene and ethylene) and carbon black [1,3]. C<sub>2</sub> compounds can be considered one of the main goals of methane pyrolysis as they are important precursors of many organic compounds [4]. Conventionally, these compounds are produced from crude oil in a process (usually steam cracking) that produces high quantities of CO<sub>2</sub>. Considering the limited availability and resources of crude oil and the inevitable production of CO<sub>2</sub>, plasma methane pyrolysis seems a much more sustainable solution. While the conventional methane resources, i.e., natural gas, are also limited, especially now, there are other possible sources. One of them is biomethane. The other one might be synthetic CH<sub>4</sub> produced from CO<sub>2</sub> [5]. While the latter possibility is to be available in the future rather than right now, it suggests an interesting combination. CO<sub>2</sub> sequestered from the atmosphere can be reduced to methane and further transformed into C<sub>2</sub> compounds that can be used in the production of polymers. As a result, CO<sub>2</sub> would be bound in a plastic material that can be used for decades or recycled.

While the methods most commonly considered for methane pyrolysis involve catalysts or molten metals and salts [6,7], they are usually focused on hydrogen and carbon black production, not C<sub>2</sub> compounds. In the case of plasma methods, the warm plasma (e.g., gliding arc plasma or microwave plasma) seems most suitable [8]. This type of plasma provides high temperatures (1000–6000 K) and the presence of reactive species (e.g., radicals) [9,10]. Both factors are crucial for the conversion of hydrocarbons. On the contrary, typical cold plasmas, e.g., dielectric barrier discharge (DBD), work usually at low temperatures resulting in low conversion. On the other hand, hot plasmas (e.g., arc plasma) provide temperatures much higher than necessary (eg, 11,000 K [11]) resulting in energy losses.

Methane decomposition requires a high temperature and is a gradual process that may lead to many products, as presented in a simplified reaction (1):



The distribution of the products depends on the temperature and reaction time. With the increase in these two parameters, acetylene, soot, and hydrogen start to dominate [12,13], with the latter two products being the final if the conditions are severe enough. Regardless of the final products, the initial step in methane decomposition is the detachment of H atom (2), which has high activation energy and determines the rate of the reaction [14,15]:



The released H radicals play a key role [9] in the further decomposition of methane, accelerating the process (3) [13,16]:



Interestingly, some of the research proved that mixing hydrogen with methane may be beneficial to the conversion of the latter and may affect the selectivity of the products. It should be noted that since methane decomposition produces hydrogen, overall the process could be considered a quasi-autocatalytic process in which part of the produced hydrogen could be returned to the process to improve its efficiency. This effect has been reported or suggested only in the case of warm plasma (e.g., microwave (MW) or gliding arc plasmas) [17–20]. In the case of traditional pyrolysis or strictly non-equilibrium plasmas, the observed effect is the opposite—the addition of hydrogen decreases the conversion rate due to reaction reversal of reaction (3), which is favored in temperatures lower than ca. 2000 K [21,22].

The effect of hydrogen addition on methane pyrolysis in warm plasmas is still an object of debate. Most researchers suggest that the key role is played by the H radicals generated in plasma [18–20]. It is speculated that their presence increases the conversion rate of methane (as in Equation (3)). Another observed effect of hydrogen addition is increases in the yield and selectivity of C<sub>2</sub>H<sub>4</sub> and C<sub>2</sub>H<sub>2</sub>. However, some discrepancies are indicated when the effect of specific H<sub>2</sub>:CH<sub>4</sub> ratio is considered. For instance, Ref. [20] shows that the beneficial effect of H<sub>2</sub> addition is observed for the maximum H<sub>2</sub>:CH<sub>4</sub> ratio of 2. Above that ratio, methane conversion rate and C<sub>2</sub> compound yield start decreasing. In opposite, work [19] shows that the increase in conversion rate and yield is observed even at the H<sub>2</sub>:CH<sub>4</sub> ratio of 5. Additionally, it should be noted that none of these works presents results of plasma diagnosis. Yet the results of such a diagnosis could be very valuable, as knowing the temperature of plasma and identifying plasma radicals should support any speculation on the hydrogen influence mechanism.

In the context of the aforementioned articles, this work aims to analyze the process of H<sub>2</sub>/CH<sub>4</sub> plasma pyrolysis in a well-diagnosed atmospheric microwave plasma reactor. The reactor in this work has a typical construction that is used by many researchers [23–25]. Most importantly, it was tested in a wide range of conditions [10,26,27]. In distinction

from other work, we were able to proof the presence of H radicals and to determine the temperature profile in the reactor (See: Section 3 Materials and Methods). This data allows the analyzing the hypotheses for conversion and selectivity changes due to H<sub>2</sub> addition. Moreover, this work provides an initial insight into the hydrogen impact on the soot particle size. Another novel aspect of this work is the investigation of nitrogen's potential to inhibit the process of soot formation.

## 2. Results and Discussion

Table 1 presents the volumetric concentrations of the inlet and outlet gases during MW plasma treatment for runs with different H<sub>2</sub>:CH<sub>4</sub> ratios. Based on these results, conversion rate, selectivities, and yield were calculated, according to Equations (17)–(21). In addition to C<sub>2</sub>H<sub>2</sub>, C<sub>2</sub>H<sub>4</sub>, and hydrogen, another main product was carbonaceous material. This material was deposited on the reactor walls as well as carried with the gas. The exact reaction mechanisms and the characteristics of solid carbon are still debated. For simplicity, the material will be referred to as soot. Methane decomposition in MW plasma can additionally result in other products, mainly C<sub>3</sub>–C<sub>4</sub> unsaturated compounds as detected on GC/MS analysis within our previous research [26]. However, the concentration of these species was negligible.

**Table 1.** Inlet and outlet concentrations of the main gaseous compounds.

H <sub>2</sub> :CH <sub>4</sub> Ratio	[CH <sub>4</sub> ] <sub>in</sub>	[CH <sub>4</sub> ] <sub>out</sub>	[H <sub>2</sub> ] <sub>in</sub>	[H <sub>2</sub> ] <sub>out</sub>	[C <sub>2</sub> H <sub>4</sub> ] <sub>out</sub>	[C <sub>2</sub> H <sub>2</sub> ] <sub>out</sub>
	%					
4:1 N <sub>2</sub> *	4.83 ± 0.04	0.39 ± 0.04	20.6 ± 1.7	27.9 ± 1.2	0.10 ± 0.02	1.11 ± 0.10
4:1 Ar *	5.12 ± 0.04	0.22 ± 0.04	19.0 ± 1.2	22.7 ± 1.2	0.11 ± 0.02	1.74 ± 0.10
3:1 Ar	5.03 ± 0.04	1.41 ± 0.04	14.2 ± 1.2	16.1 ± 1.2	0.09 ± 0.01	1.24 ± 0.10
2:1 Ar	4.99 ± 0.04	1.69 ± 0.04	8.7 ± 1.2	11.3 ± 1.2	0.08 ± 0.01	1.05 ± 0.10
1:1 Ar	5.08 ± 0.04	2.35 ± 0.04	4.4 ± 1.2	6.8 ± 1.2	0.08 ± 0.01	0.85 ± 0.10
0:1 Ar	4.92 ± 0.04	1.32 ± 0.04	0.0 ± 0.0	4.6 ± 1.2	0.08 ± 0.01	0.99 ± 0.10

\* Indicates the diluent.

### 2.1. Methane Conversion

The influence of H<sub>2</sub>:CH<sub>4</sub> ratio on methane conversion (for the test with Ar as diluent) is presented in Figure 1. We observe a considerable decrease in X<sub>CH<sub>4</sub></sub> when H<sub>2</sub>:CH<sub>4</sub> ratio increases from 0:1 to 1:1. This is in opposition to what we reported in our previous work [18] where the addition of hydrogen had positive effect for H<sub>2</sub>:CH<sub>4</sub> ratio of 1:1 and even 1:3. Moreover, in work [19], a gradual increase in H<sub>2</sub>:CH<sub>4</sub> ratio from 1:5 to 1:1 also showed positive effects on CH<sub>4</sub> conversion. The reason for these different results is probably the diluent. In case of the two aforementioned works, no diluent was applied. In the present work, Ar was used. While Ar does not undergo chemical reaction, it may take part in energy-transition-initiating decomposition reactions. In fact, long-living metastable excited Ar particles carrying high energy are known to initiate the decomposition of organic compounds [27], as in Equation (4):



The addition of hydrogen may lead to collision with hydrogen molecules instead of CH<sub>4</sub>, resulting in the quenching of Ar-excited molecules [28], as in Equations (5) and (6):



Therefore, it may be speculated that with the presence of hydrogen and argon, two decomposition pathways compete, one involving H radical (Equation (3)) and the other metastable Ar particle (Equation (4)). With the H<sub>2</sub>:CH<sub>4</sub> ratio of 1:1, the amount of hydrogen is enough to quench some of the Ar\* particles. At the same time, the number of produced H radicals is not enough to compensate the loss in methane conversion due to metastable argon quenching. Therefore, a drop in CH<sub>4</sub> conversion is observed when compared with Ar-CH<sub>4</sub> mixture. With the increase in H<sub>2</sub> concentration, more H radicals are produced, resulting in the improvement of methane conversion when the applied ratio is 4:1. It should be emphasized that the presence of H radicals was proven in the upper plasma zone (in the place of plasma ignition) in previous research on the same reactor with very similar process conditions [10,26]. Therefore, it can be assumed that in the high-temperature upper part of the reactor (see Section 3 Materials and Methods), the addition of hydrogen results in H radical generation that can enhance methane decomposition.

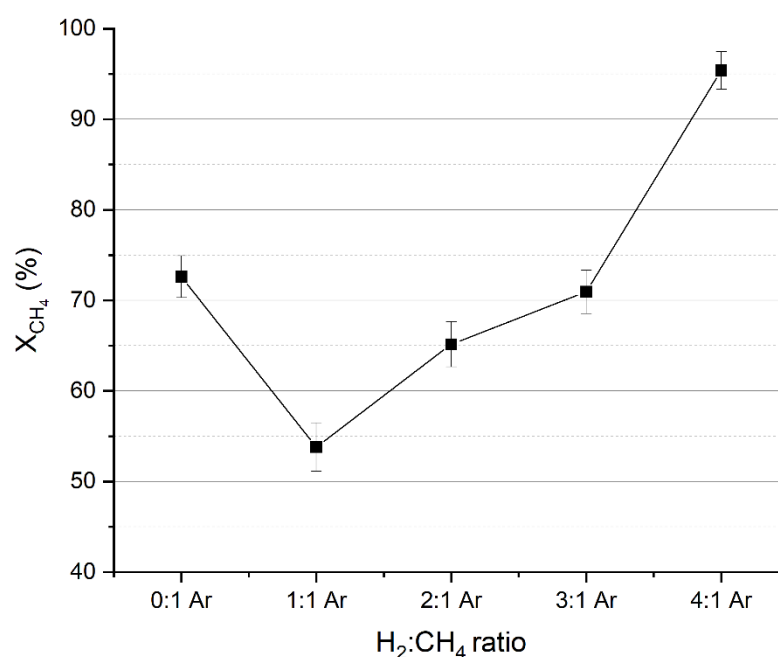


**Figure 1.** Influence of H<sub>2</sub>:CH<sub>4</sub> ratio on methane conversion rate (in Ar dilution).

## 2.2. C<sub>2</sub> Compounds Selectivity and Yield

In addition to influencing methane conversion, the addition of hydrogen also influences products' yield and selectivity. Figure 2 presents the changes in the C<sub>2</sub>H<sub>2</sub> yield and selectivity in correlation to H<sub>2</sub>:CH<sub>4</sub> ratio. Opposite to X<sub>CH<sub>4</sub></sub>, the trend is more straightforward when considering C<sub>2</sub>H<sub>2</sub>. The drop in case 1:1 is a result of a significant decrease in CH<sub>4</sub> conversion (see Figure 1). In all other cases with H<sub>2</sub> addition, the C<sub>2</sub>H<sub>2</sub> yield increases mainly due to increases in its selectivity but also thanks to a higher conversion rate (case 4:1). The increase in C<sub>2</sub>H<sub>2</sub> selectivity is probably caused by the inhibition of acetylene conversion to heavier products, e.g., soot and aromatics [18,26]. In the case of C<sub>2</sub>H<sub>4</sub>, the results are not as linear as in the case of C<sub>2</sub>H<sub>2</sub> (Figure 3). In a high temperature of the plasma, C<sub>2</sub>H<sub>2</sub> production is favored over C<sub>2</sub>H<sub>4</sub>, resulting in a much lower concentration of the latter. As a result, the measurements are much less reliable and burdened with a high error. Therefore, it is hard to analyze the obtained trends in detail. Nevertheless, there is a noticeable and quite clear increase in both the selectivity and yield of C<sub>2</sub>H<sub>4</sub> when H<sub>2</sub> is added. It should be noted that the formation of C<sub>2</sub> compounds takes place in the lower part of the reactor where the temperature varies in range of 1000 K (See Section 3 Materials and Methods). In this region, the role of hydrogen addition is different than in the upper part of the reactor. Instead of methane conversion due to the presence of H radicals, the H<sub>2</sub> molecules shifts the distribution of the products towards C<sub>2</sub> compounds.

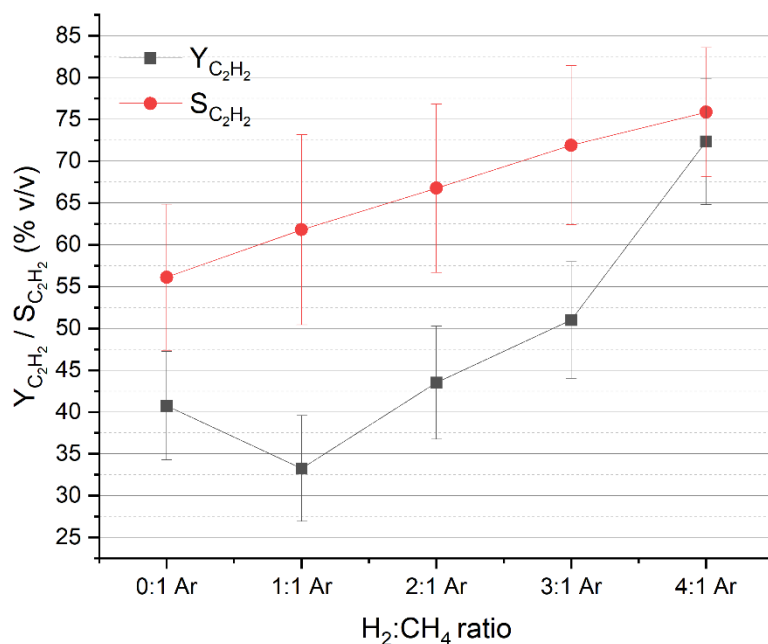


Figure 2. H<sub>2</sub> impact on C<sub>2</sub>H<sub>2</sub> selectivity and yield.

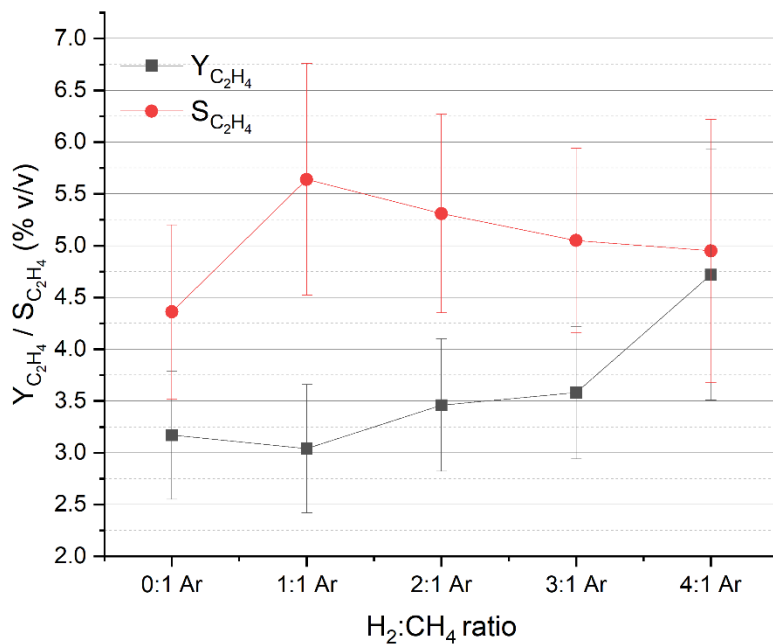
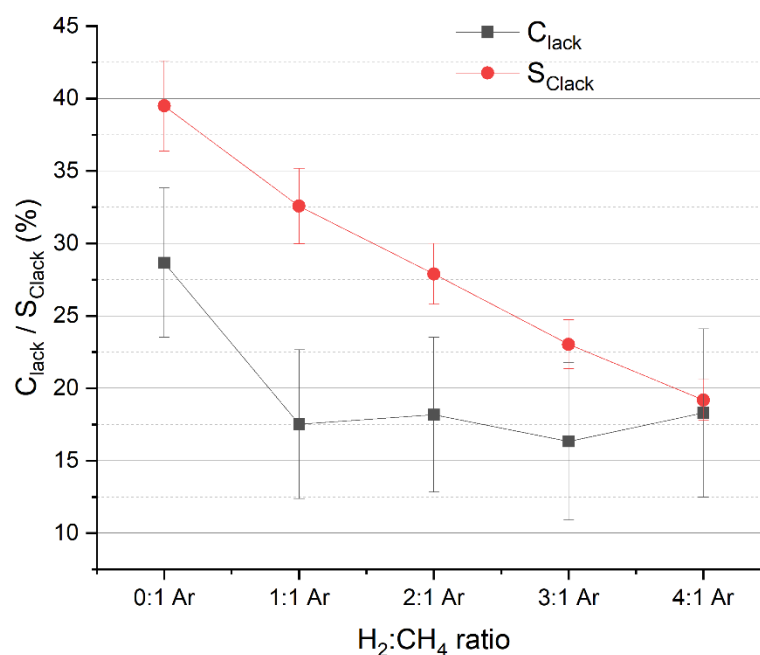


Figure 3. H<sub>2</sub> impact on C<sub>2</sub>H<sub>4</sub> selectivity and yield.

### 2.3. Soot

The effect of hydrogen addition on the soot quantity can be evaluated based on the balance of carbon. In the discussed case carbon lack ( $C_{\text{lack}}$ —Equation (20)) can be equated with soot yield. This assumption neglects possible small amounts of aromatics and C<sub>3</sub>–C<sub>4</sub> products. Carbon lack along with its selectivity (which can be treated as soot selectivity) are presented in Figure 4.  $C_{\text{lack}}$  drops significantly when hydrogen is added. The precise impact of different H<sub>2</sub>:CH<sub>4</sub> ratios on  $C_{\text{lack}}$  is hard to determine as the error of these parameters (resulting from the carbon balance that involves many variables) is relatively high. However, the trend of the selectivity drop is much more reliable. Its gradual decrease is an outcome of a quite stable  $C_{\text{lack}}$  and increase in CH<sub>4</sub> conversion. In other words, with the addition of hydrogen, the amount of produced soot is more or less the same regardless of H<sub>2</sub>:CH<sub>4</sub>

ratio. On the other hand, with increasing ratio, more methane is converted, which should produce more soot. Since it is not, the selectivity of soot drops, suggesting the inhibition of soot formation. As mentioned, the addition of hydrogen inhibits processes leading to the transformation of acetylene into aromatic and soot [18,26]. This can be explained by the termination of aromatic radicals ( $A_{i-}$ ), as in Equation (7), that otherwise would react with acetylene (Equation (8)), leading to the densification of aromatic structure that eventually results in soot formation (as in HACA mechanism).



**Figure 4.** Changes in soot yield and selectivity with the increase of H<sub>2</sub>:CH<sub>4</sub> ratio.

The decrease in the amount of soot formed during the process was also observed visually as the reactor's quartz tube was remaining transparent longer and the amount of the soot sample that was collected from the tube was the smallest for the runs with the highest H<sub>2</sub>:CH<sub>4</sub> ratio. The influence of hydrogen addition on lowering soot output was also confirmed in other research [18,19]

It is hypothesized that the addition of hydrogen can also affect the soot characteristics. In the previous work [18], this assumption was based on the calculated C and H lack as well as H<sub>2</sub> selectivity. Since hydrogen may inhibit the formation of soot derived from aromatics (as in HACA mechanism), the produced carbonaceous material should include a higher share of carbon material that was formed directly from CH<sub>4</sub> decomposition in high-temperature plasma region. Within this experiment, we performed SEM analysis to investigate possible differences in the particle sizes of the formed soot depending on the addition of H<sub>2</sub>. Two exemplary SEM pictures along with the particles size distributions are shown in Figures 5 and 6. Analyzing the particle size distribution, it is clear that the addition of hydrogen results in a higher share of bigger particles. For a H<sub>2</sub>:CH<sub>4</sub> ratio of 4:1, a larger share of large particles (size up to  $r_p \approx 400 \mu\text{m}$ ) was detected. On the other hand, if no H<sub>2</sub> is added to the inlet gas stream, smaller particles are more dominant (59% for the ratio of 0:1 compared to 54% for ratios from 1:1 to 3:1 and 43% for the ratio of 4:1). We hypothesize that the increase in the particles size (due to hydrogen addition) might be caused by the aforementioned changes in the carbonaceous material nature and origin. While this is yet another premise suggesting that the hydrogen addition may impact

the characteristics of soot, more analyses and data are necessary as the reason for this phenomenon is still unknown. However, the beneficial outcome of this phenomenon would be an easier separation of the particles from the gas stream, regardless of whether it would be a valuable product or an unwanted byproduct.

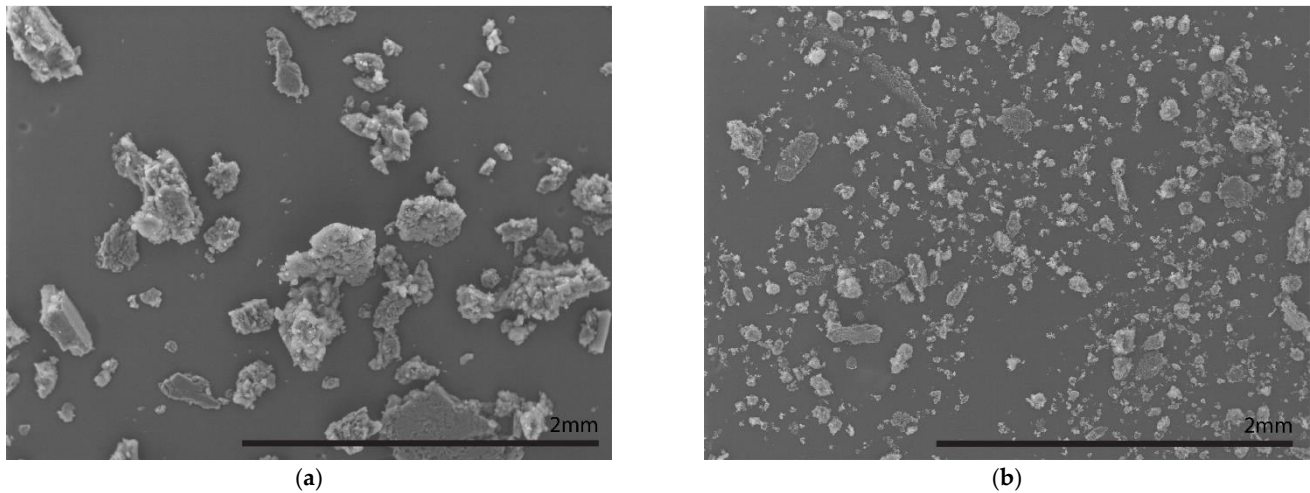


**Figure 5.** Soot's SEM pictures for the  $H_2:CH_4$  ratio of 4:1 (a) and 0:1 (b).

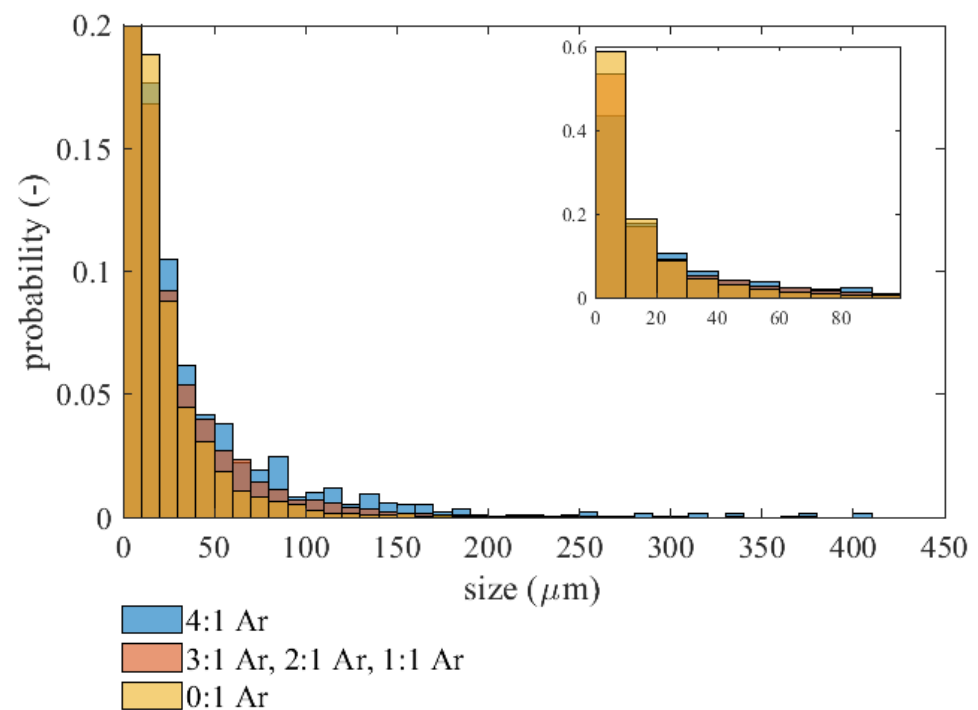


**Figure 6.** Particle size distribution of carbon powders resulting from different  $H_2:CH_4$  ratio, after extraction from the reactor.

#### 2.4. Hydrogen

It should be noted that the hydrogen added to the process is not consumed. However, since it shifts products distribution towards  $C_2$  compounds, less hydrogen might be produced when compared with the most-harsh condition pyrolysis aiming for  $H_2$  production and leading to the co-production of carbon black (see Equation (1)). This phenomenon is shown in Figure 7 presenting yield and selectivity of hydrogen (the selectivity of hydrogen should be considered separately to the carbon-based selectivities, i.e.,:  $S_{C_2H_2}$ ,  $S_{C_2H_4}$ ,  $C_{lack}$ ). It should be noted that in the case of  $H_2:CH_4$  ratio of 4, the yield of  $H_2$  is close to the

case with no hydrogen addition. This is due to the increase in methane conversion. In other words, while the selectivity of  $H_2$  drops with hydrogen co-feeding, the wastage of the amount of produced hydrogen might be compensated by the improved methane conversion and higher output of the products.

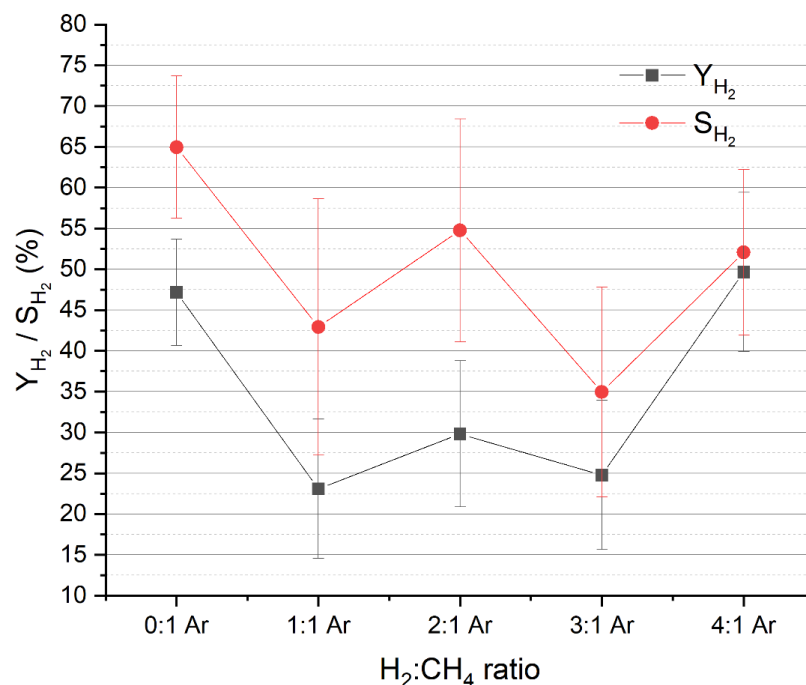


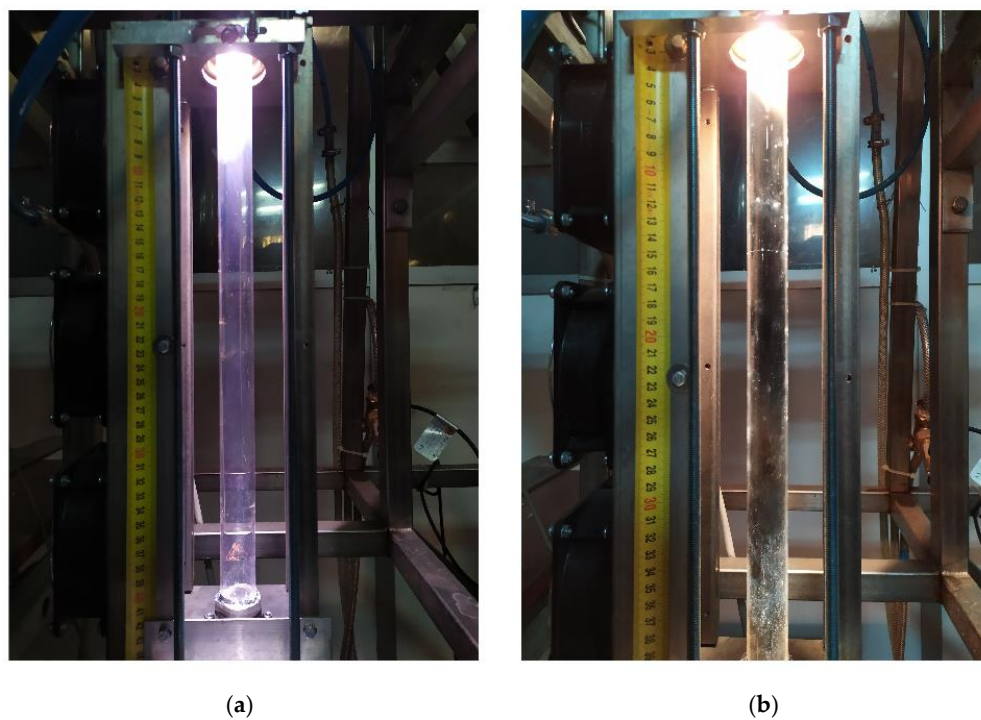
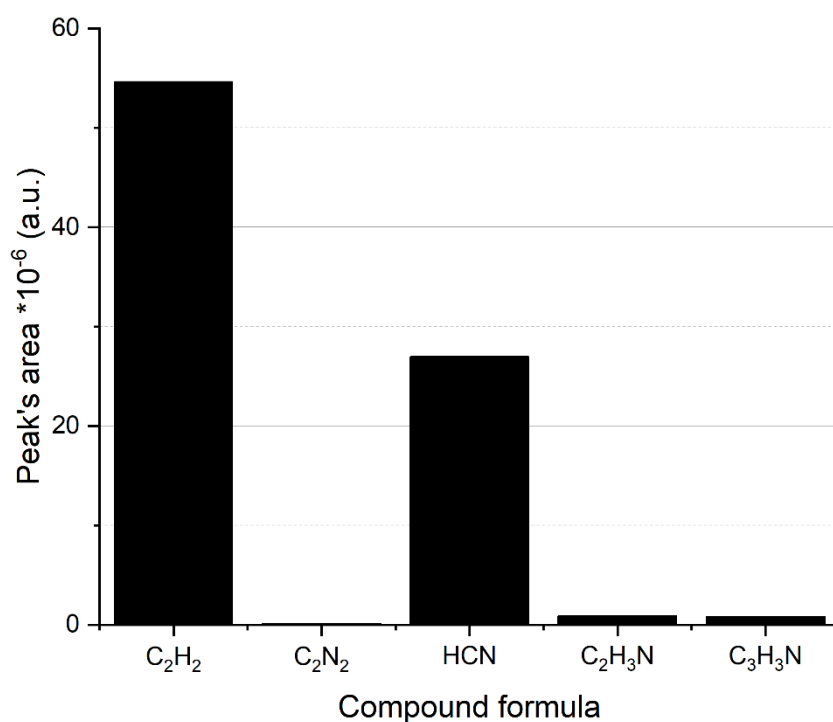
**Figure 7.** Changes in hydrogen yield and selectivity depending on  $H_2:CH_4$  ratio.

### 2.5. Influence of Nitrogen Addition

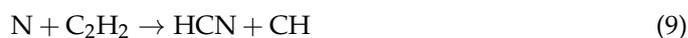
The addition of nitrogen can affect soot formation, as proven in one of the previous works considering MW application in producer gas valorization [26]. In this work, this issue is given more attention by comparing two runs with different diluents: Ar or  $N_2$ , with both cases applying the  $H_2:CH_4$  ratio of 4:1. Results from these tests are compared in Table 2. With  $N_2$  addition, a slight decrease in methane conversion was observed. A much more significant drop was observed for  $C_2H_2$  selectivity and yield. On the other hand,  $C_2H_4$  production was not affected by the  $N_2$  addition. However, the main difference between the two tests is the fact that with  $N_2$  addition, no soot was produced. Any soot deposition was quite easily observed on the quartz tube of the reactor, and this happened in all the cases with Ar as the diluent. With  $N_2$  testing, no deposit was observed. This is visualized in Figure 8. It should be noted that with no soot, the C lack and its selectivity describe the carbon–nitrogen compounds that are produced due to nitrogen addition. It should be noted that this is in contrary to the tests with Ar. These carbon–nitrogen compounds were confirmed in our previous research with almost identical conditions applied (1800 W, 30 L/min,  $CH_4$ —4%,  $H_2$ —8%,  $N_2$ —rest) [10]. The results from the GC/MS analysis of these compounds are presented in Figure 9. It should be noted that this results present only area of the chromatogram’s peaks. The correlation between the peak’s area and the real concentration is usually different for different compounds. However, the size of the peaks is enough to estimate which compounds dominate and if their amount is within the same range. Therefore, while the analysis confirmed presence of  $C_2$ – $C_3$  nitrogen-containing compounds (i.e., cyanogen, acetonitrile, acrylonitrile) their concentration is negligible when compared to HCN. Besides nitrogen compounds, the figure also includes acetylene. This allows estimating that the concentration of  $C_2H_2$  and HCN is more or less within the same range and such a conclusion is in good agreement with  $C_{lack}$  (indicating yield of carbon-nitrogen compounds that were not quantified) and  $Y_{C_2H_2}$  (Table 2).

**Table 2.** Nitrogen impact on the process parameters.

Run	$X_{CH_4}$	$Y_{C_2H_2}$	$Y_{C_2H_4}$	$S_{C_2H_2}$	$S_{C_2H_4}$	$C_{lack}$	$S_{Clack}$
4:1 N <sub>2</sub>	91.5 ± 2.4	49 ± 13	4.5 ± 1.4	53 ± 14	4.9 ± 1.5	38.5 ± 7.4	42.1 ± 5.2
4:1 Ar	95.4 ± 2.1	72 ± 10	4.7 ± 1.2	76 ± 11	5.0 ± 1.3	18.3 ± 5.8	19.2 ± 1.4

**Figure 8.** The quartz tube of the reactor during tests 4:1 N<sub>2</sub> (a) and 4:1 Ar (b).**Figure 9.** Nitrogen-containing compounds detected in the outlet gas (with C<sub>2</sub>H<sub>2</sub> as reference).

The formation of HCN can be explained by the interaction of acetylene and  $C_xH_y$  radicals with nitrogen molecules and radicals [29–31] as in reactions (9)–(12):



It should be noted that nitrogen radicals were confirmed within the plasma in similar conditions [10]. This would explain why the concentration of acetylene decreased so significantly when  $N_2$  was added. The consumption of  $C_2H_2$  and hydrocarbon radicals in HCN formation might be competitive with soot formation and could have resulted in a decrease in the amount of produced soot. However, previous research showed that in  $CH_4/N_2$  mixtures both soot and HCN were observed [26]. Therefore, it might be concluded that both  $N_2$  and  $H_2$  are necessary to inhibit soot formation to a higher degree. In that case, one of the possible explanations would involve NH radicals and their reaction with  $CH_2$  and CH radicals [29], as in (13)–(14):



The NH radicals are formed in a high-temperature region of  $N_2/H_2$  MW plasma [26]. The interaction between NH and  $C_xH_y$  radicals could have been another way of inhibiting soot formation due to  $C_xH_y$  radicals consumption that otherwise would take part in the chain growth of soot. Finally, the other possible explanation might be a transformation of the already produced soot into HCN. This phenomenon was observed in the work of Orikasa and Tomita [32] and is explained by the interaction between nitrogen contained on the surface of carbonaceous material and  $H_2$  and/or H, as presented in reaction (15):



It should be noted that the soot formed from hydrocarbons in nitrogen MW plasma does include nitrogen in its structures [33], which is necessary for this mechanism to occur. Moreover, in opposite to the two previous mechanisms that would inhibit soot formation, the latter one would convert already produced soot. Finally, the three discussed mechanisms do not exclude each other, and it is possible that all of them have their share in the discussed phenomenon.

### 3. Materials and Methods

The tests were carried out in the MW plasma reactor that is described in detail in previous research [10,27,28]. Briefly, the power of microwaves initiating and sustaining the plasma is ca. 1800 W. The processed gas acts as a plasma agent and is introduced into the reactor tangentially resulting in a swirl flow. The plasma is generated in the reactor's quartz tube. It should be noted that while the plasma was not diagnosed for the purpose of the presented results, it was thoroughly investigated previously for very similar conditions [10,27,28]. It was shown that the temperature of the plasma core near the spot of plasma ignition is close to 4000–6000 K, and it drops along the reactor, reaching 1000–1200 K at the bottom of the quartz tube. Therefore, two temperatures zones can be distinguished: a short (up to 10 cm) high-temperature zone and a long (ca. 50 cm) lower-temperature zone. It should be noted that the gases are introduced above the ignition zone and their pass through both of the temperatures zones.

The whole experimental setup is shown in Figure 10. The tests were done with a fixed total gas flow rate of 30 L/min and a fixed microwave power of ca. 1800 W. The process gas

consisted of a mixture of methane, a dilution gas and optionally H<sub>2</sub>. While the tests were normally performed with an Ar dilution, another analyzed variation involved N<sub>2</sub> instead of Ar. Both of these gases were necessary to sustain the plasma that tends to quench when a high concentration of H<sub>2</sub> and CH<sub>4</sub> is applied (due to increased reflection of microwaves). The ratio of H<sub>2</sub>:CH<sub>4</sub> was changed in the range of 0:1 (no hydrogen) to 4:1, with the CH<sub>4</sub> concentration being constant and equal to ca. 5% *v/v*. The flow rates of all the gases (H<sub>2</sub>, CH<sub>4</sub>, Ar, and N<sub>2</sub>) were controlled with the use of rotameters. The concentration of Ar was used to determine changes in the volumetric gas flow rate due to gas processing and resulting chemical reactions. As argon does not undergo chemical reactions, changes of its concentration are result of the changes in the volumetric gas flow rate. Therefore, a small stream of Ar (ca. 7% *v/v*) was used even when nitrogen was the main diluent. At the outlet of the reactor, the gas samples were probed into Tedlar's bags and analyzed by GC (gas chromatography) techniques with the use of Agilent 7820 (TCD detector) and HP 6890 (FID detector). More details on the GC analyses are given in Table 3.

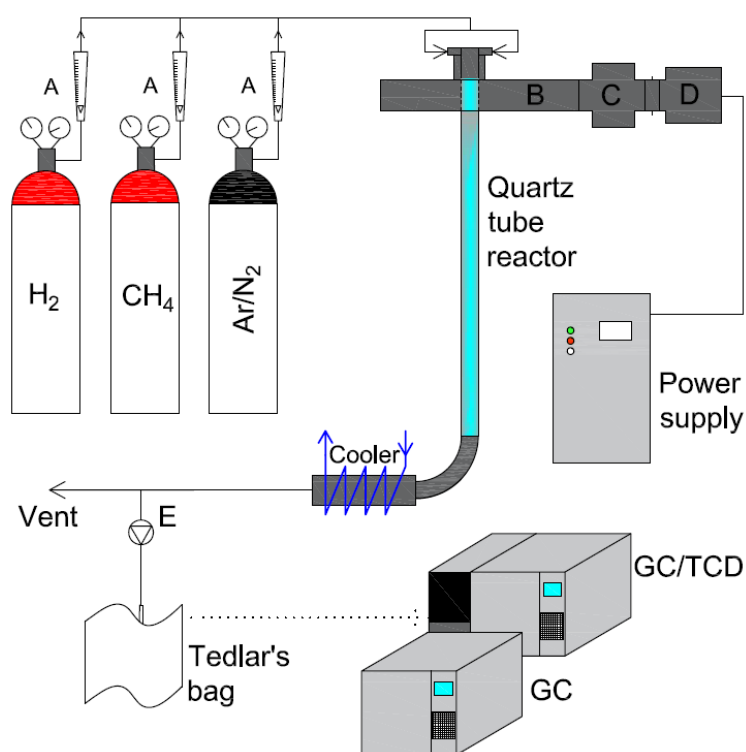


**Figure 10.** Scheme of the test rig. A—rotameters, B—MW plasma reactor's waveguide, C—MW plasma reactor's circulator and reflectometer, D—MW plasma reactor's generator, E—diaphragm pump.

**Table 3.** Parameters of the GC analyses.

Analyzed Compound	Detector	Column	Temperature
CH <sub>4</sub> , C <sub>2</sub> H <sub>2</sub> , C <sub>2</sub> H <sub>4</sub>	FID	RT-Alumina BOND/KCl	100 °C (3 min)
H <sub>2</sub> , CO, Ar	TCD	HP-Molesieve	45 °C (4 min) $\xrightarrow{10\text{ }^{\circ}\text{C}/\text{min}}$ 100 °C

The soot produced during the tests was collected from the reactor's quartz tube. Three samples were collected: from the test with the H<sub>2</sub>:CH<sub>4</sub> ratio of 0:1, from the test with the ratio of 4:1, and a collective sample from tests with H<sub>2</sub>:CH<sub>4</sub> ratio from 1:1 to 3:1. Scanning microscopy images of the carbon powder were captured with a Hitachi TM3030Plus, at 15 kV, a working distance of 10.70 mm, and with a mixed signal from the backscattered and secondary electrons. Particle size distribution was determined using ImageJ. In the first step, the image was binarized using a threshold selected visually to correctly capture

particles while ignoring the background. Then the particle analyzer feature of ImageJ was used to give a list of detected particles and their area. The corresponding particle radius was calculated as  $r_p \approx \sqrt{A}$  (assuming spherical particles).

As toxic hydrogen cyanide was expected to be produced in the tests with nitrogen addition, the outlet of the reactor was connected to the vent. Additionally, an HCN detector (Dräger Pac 8000) was available at the test rig.

To evaluate the process of methane pyrolysis, the following parameters were determined:  
Outlet volumetric gas flow rate:

$$v_{out} \left( \frac{\text{L}}{\text{min}} \right) = v_{in} \times \frac{[\text{Ar}]_{in}}{[\text{Ar}]_{out}} \quad (16)$$

where  $v_{in}$ —inlet volumetric gas flow rate (L/min),  $[\text{Ar}]_{in}$ —inlet argon concentration (% v/v),  $[\text{Ar}]_{out}$ —outlet argon concentration (% v/v).

Methane conversion rate:

$$X_{\text{CH}_4} (\%) = \left( 1 - \frac{[\text{CH}_4]_{out} \times v_{out}}{[\text{CH}_4]_{in} \times v_{in}} \right) \times 100 \quad (17)$$

where  $[\text{CH}_4]_{out}$ —outlet methane concentration (% v/v),  $[\text{CH}_4]_{in}$ —inlet methane concentration (% v/v).

Selectivity (carbon-based) of C<sub>2</sub> compounds (acetylene, ethylene):

$$S_{\text{C}_x\text{H}_y} (\%) = \left( \frac{x \times [\text{C}_x\text{H}_y]_{out} \times v_{out}}{[\text{CH}_4]_{in} \times v_{in} - [\text{CH}_4]_{out} \times v_{out}} \right) \times 100 \quad (18)$$

where  $x$ —number of molecule's carbon atoms,  $[\text{C}_x\text{H}_y]_{out}$ —outlet concentration of C<sub>2</sub> compounds.

Yield of C<sub>2</sub> compounds (acetylene, ethylene):

$$Y_{\text{C}_x\text{H}_y} (\%) = \frac{X_{\text{CH}_4} \times S_{\text{C}_x\text{H}_y}}{100} \quad (19)$$

Carbon lack, which is defined as the difference between the quantified amounts of inlet and outlet carbon in gaseous species:

$$C_{lack} (\%) = \left( 1 - \frac{v_{out} \times \sum (x \times [\text{C}_x\text{H}_y]_{out}) + v_{out} \times [\text{CH}_4]_{out}}{[\text{CH}_4]_{in} \times v_{in}} \right) \times 100 \quad (20)$$

Selectivity of carbon lack:

$$S_{Clack} (\%) = \frac{C_{lack} (\%)}{X_{\text{CH}_4} (\%)} \times 100 \quad (21)$$

Hydrogen selectivity:

$$S_{\text{H}_2} (\%) = \left( \frac{1}{2} \times \frac{[\text{H}_2]_{out} \times v_{out} - [\text{H}_2]_{in} \times v_{in}}{[\text{CH}_4]_{in} \times v_{in} - [\text{CH}_4]_{out} \times v_{out}} \right) \times 100 \quad (22)$$

Hydrogen yield:

$$Y_{\text{H}_2} (\%) = \frac{X_{\text{CH}_4} (\%) \times S_{\text{H}_2} (\%)}{100} \quad (23)$$

#### 4. Conclusions

The paper presents an investigation of the impact of hydrogen addition on methane pyrolysis in microwave plasma with the main focus given to C<sub>2</sub> compounds and soot products rather than hydrogen. It shows that hydrogen presence influences all aspects of methane pyrolysis. Applying H<sub>2</sub>:CH<sub>4</sub> ratio of 4:1 results in the increase of methane

conversion from ca. 72% (for the case with no hydrogen addition) to 95%. The yields of  $C_2H_2$  and  $C_2H_4$  increase from ca. 41% to 72%, and from 3.2% to 4.7%, respectively. Similarly, the selectivity increases from ca. 56% to 75%, and from 4.3% to 5.0%, for  $C_2H_2$  and  $C_2H_4$  respectively. At the same time, addition of hydrogen leads to decreases in the yield (from ca. 28% to 18%) and selectivity (from ca. 40% to 18%) of soot and increase the size of soot particles. Interestingly, while an increasing trend of  $CH_4$  conversion towards high ratios of  $H_2:CH_4$  is observed a minimum is reached at  $H_2:CH_4$  1:1. This conversion drop is probably caused by quenching of metastable Ar particles that otherwise play an important role in initiating methane decomposition. Further investigations are necessary to determine the global impact of hydrogen addition on the process efficiency. Nevertheless, the results show that hydrogen addition might be a promising approach for a methane pyrolysis process focused on  $C_2$  compounds formation. Moreover, one aspect is of high technical relevance—the soot formation. The inhibition of soot formation due to hydrogen presence might be important for methane pyrolysis. The amount of soot produced if methane pyrolysis becomes a full-scale commercial process would be far above the global demand, resulting in a stream of problematic waste rather than a valuable product [1]. In that context, this paper shows that one possible solution is the addition of nitrogen. With the presence of nitrogen and hydrogen, the formation of soot was completely stopped. Instead of soot, hydrogen cyanide formed. The possibility of switching between soot and HCN as one of the products, along with improved  $CH_4$  conversion and higher selectivity of  $C_2$  compounds, would surely make methane pyrolysis more flexible and attractive.

**Author Contributions:** Conceptualization, M.W.; methodology, M.W.; validation, M.W. and J.G.; formal analysis, M.W., J.G. and K.M.; investigation, K.M., M.W. and J.G.; resources, M.W.; writing—original draft preparation, M.W.; writing—review and editing, J.G.; visualization, M.W. and J.G.; supervision, M.W. All authors have read and agreed to the published version of the manuscript.

**Funding:** This research received no external funding.

**Institutional Review Board Statement:** Not applicable.

**Informed Consent Statement:** Not applicable.

**Data Availability Statement:** Not applicable.

**Conflicts of Interest:** The authors declare no conflict of interest.

## References

1. Sánchez-Bastardo, N.; Schlögl, R.; Ruland, H. Methane Pyrolysis for Zero-Emission Hydrogen Production: A Potential Bridge Technology from Fossil Fuels to a Renewable and Sustainable Hydrogen Economy. *Ind. Eng. Chem. Res.* **2021**, *60*, 11855–11881. [[CrossRef](#)]
2. Cheon, S.; Byun, M.; Lim, D.; Lee, H.; Lim, H. Parametric Study for Thermal and Catalytic Methane Pyrolysis for Hydrogen Production: Techno-Economic and Scenario Analysis. *Energies* **2021**, *14*, 6102. [[CrossRef](#)]
3. Riley, J.; Atallah, C.; Siriwardane, R.; Stevens, R. Technoeconomic analysis for hydrogen and carbon Co-Production via catalytic pyrolysis of methane. *Int. J. Hydrogen Energy* **2021**, *46*, 20338–20358. [[CrossRef](#)]
4. Minea, T.; van den Bekerom, D.C.M.; Peeters, F.J.J.; Zoethout, E.; Graswinckel, M.F.; van de Sanden, M.C.M.; Cents, T.; Lefferts, L.; van Rooij, G.J. Non-oxidative methane coupling to  $C_2$ hydrocarbons in a microwave plasma reactor. *Plasma Process. Polym.* **2018**, *15*, 1800087. [[CrossRef](#)]
5. Li, L.; Zeng, W.; Song, M.; Wu, X.; Li, G.; Hu, C. Research Progress and Reaction Mechanism of  $CO_2$  Methanation over Ni-Based Catalysts at Low Temperature: A Review. *Catalysts* **2022**, *12*, 244. [[CrossRef](#)]
6. Msheik, M.; Rodat, S.; Abanades, S. Methane Cracking for Hydrogen Production: A Review of Catalytic and Molten Media Pyrolysis. *Energies* **2021**, *14*, 3107. [[CrossRef](#)]
7. Sánchez-Bastardo, N.; Schlögl, R.; Ruland, H. Methane Pyrolysis for  $CO_2$ -Free  $H_2$  Production: A Green Process to Overcome Renewable Energies Unsteadiness. *Chem. Ing. Tech.* **2020**, *92*, 1596–1609. [[CrossRef](#)]
8. Heijkers, S.; Aghaei, M.; Bogaerts, A. Plasma-Based  $CH_4$  Conversion into Higher Hydrocarbons and  $H_2$ : Modeling to Reveal the Reaction Mechanisms of Different Plasma Sources. *J. Phys. Chem. C* **2020**, *124*, 7016–7030. [[CrossRef](#)]
9. Zhang, H.; Wang, W.; Li, X.; Han, L.; Yan, M.; Zhong, Y.; Tu, X. Plasma activation of methane for hydrogen production in a  $N_2$  rotating gliding arc warm plasma: A chemical kinetics study. *Chem. Eng. J.* **2018**, *345*, 67–78. [[CrossRef](#)]

10. Wnukowski, M.; Jamróz, P. Microwave plasma treatment of simulated biomass syngas: Interactions between the permanent syngas compounds and their influence on the model tar compound conversion. *Fuel Process. Technol.* **2018**, *173*, 229–242. [[CrossRef](#)]
11. Mašláni, A.; Hrabovský, M.; Křenek, P.; Hlína, M.; Raman, S.; Sikarwar, V.S.; Jeremiáš, M. Pyrolysis of methane via thermal steam plasma for the production of hydrogen and carbon black. *Int. J. Hydrogen Energy* **2021**, *46*, 1605–1614. [[CrossRef](#)]
12. Cheng, Y.; Li, T.; Rehmet, C.; An, H.; Yan, B.; Cheng, Y. Detailed kinetic modeling of chemical quenching processes of acetylene-rich gas at high temperature. *Chem. Eng. J.* **2017**, *315*, 324–334. [[CrossRef](#)]
13. Scapinello, M.; Delikonstantis, E.; Stefanidis, G.D. The panorama of plasma-assisted non-oxidative methane reforming. *Chem. Eng. Process. Process Intensif.* **2017**, *117*, 120–140. [[CrossRef](#)]
14. Cuoci, A.; Frassoldati, A.; Faravelli, T.; Ranzi, E. A computational tool for the detailed kinetic modeling of laminar flames: Application to C<sub>2</sub>H<sub>4</sub>/CH<sub>4</sub> coflow flames. *Combust. Flame* **2013**, *160*, 870–886. [[CrossRef](#)]
15. Olsvik, O.; Rokstad, O.A.; Holmen, A. Pyrolysis of methane in the presence of hydrogen. *Chem. Eng. Technol.* **1995**, *18*, 349–358. [[CrossRef](#)]
16. Keramiotis, C.; Vourliotakis, G.; Skevis, G.; Founti, M.; Esarte, C.; Sánchez, N.; Millera, A.; Bilbao, R.; Alzueta, M. Experimental and computational study of methane mixtures pyrolysis in a flow reactor under atmospheric pressure. *Energy* **2012**, *43*, 103–110. [[CrossRef](#)]
17. Ma, J.; Zhang, M.; Wu, J.; Yang, Q.; Wen, G.; Su, B.; Ren, Q. Hydrolysis of n-Hexane and Toluene to Acetylene in Rotating-Arc Plasma. *Energies* **2017**, *10*, 899. [[CrossRef](#)]
18. Wnukowski, M.; van de Steeg, A.; Hrycak, B.; Jasiński, M.; van Rooij, G. Influence of hydrogen addition on methane coupling in a moderate pressure microwave plasma. *Fuel* **2021**, *288*, 119674. [[CrossRef](#)]
19. Shen, C.; Sun, D.; Yang, H. Methane coupling in microwave plasma under atmospheric pressure. *J. Nat. Gas Chem.* **2011**, *20*, 449–456. [[CrossRef](#)]
20. Zhang, J.-Q.; Yang, Y.-J.; Zhang, J.-S.; Liu, Q.; Tan, K.-R. Non-Oxidative Coupling of Methane to C<sub>2</sub> Hydrocarbons under Above-Atmospheric Pressure Using Pulsed Microwave Plasma. *Energy Fuels* **2002**, *16*, 687–693. [[CrossRef](#)]
21. Drost, H.; Klotz, H.; Schulz, G. The influence of hydrogen on the kinetics of plasmapyrolytic methane conversion. *Plasma Chem. Plasma Process.* **1985**, *5*, 55–65. [[CrossRef](#)]
22. Scapinello, M.; Delikonstantis, E.; Stefanidis, G. Direct methane-to-ethylene conversion in a nanosecond pulsed discharge. *Fuel* **2018**, *222*, 705–710. [[CrossRef](#)]
23. Chun, S.M.; Hong, Y.C.; Choi, D.H. Reforming of methane to syngas in a microwave plasma torch at atmospheric pressure. *J. CO<sub>2</sub> Util.* **2017**, *19*, 221–229. [[CrossRef](#)]
24. Czyłkowski, D.; Hrycak, B.; Miotk, R.; Jasiński, M.; Dors, M.; Mizeraczyk, J. Hydrogen production by conversion of ethanol using atmospheric pressure microwave plasmas. *Int. J. Hydrogen Energy* **2015**, *40*, 14039–14044. [[CrossRef](#)]
25. Snoeckx, R.; Bogaerts, A. Plasma technology—A novel solution for CO<sub>2</sub> conversion? *Chem. Soc. Rev.* **2017**, *46*, 5805–5863. [[CrossRef](#)] [[PubMed](#)]
26. Wnukowski, M.; Jamróz, P.; Niedzwiecki, L. The role of hydrogen in microwave plasma valorization of producer gas. *Int. J. Hydrog. Energy* **2021**, in press. [[CrossRef](#)]
27. Jamróz, P.; Kordylewski, W.; Wnukowski, M. Microwave plasma application in decomposition and steam reforming of model tar compounds. *Fuel Process. Technol.* **2018**, *169*, 1–14. [[CrossRef](#)]
28. Taghvaei, H.; Jahanmiri, A.; Rahimpour, M.R.; Shirazi, M.M.; Hooshmand, N. Hydrogen production through plasma cracking of hydrocarbons: Effect of carrier gas and hydrocarbon type. *Chem. Eng. J.* **2013**, *226*, 384–392. [[CrossRef](#)]
29. Bogaerts, A.; Gijbels, R. Effects of adding hydrogen to an argon glow discharge: Overview of relevant processes and some qualitative explanations. *J. Anal. At. Spectrom.* **2000**, *15*, 441–449. [[CrossRef](#)]
30. Oumghar, A.; Legrand, J.C.; Diamy, A.M.; Turillon, N. Methane conversion by an air microwave plasma. *Plasma Chem. Plasma Process.* **1995**, *15*, 87–107. [[CrossRef](#)]
31. Juul-Dam, T.; Brockmeier, N.F. Kinetics of Formation of Hydrogen Cyanide from Methane and Ammonia in a Microwave Plasma. *Ind. Eng. Chem. Prod. Res. Dev.* **1970**, *9*, 388–397. [[CrossRef](#)]
32. Miller, J.A.; Bowman, C.T. Mechanism and modeling of nitrogen chemistry in combustion. *Prog. Energy Combust. Sci.* **1989**, *15*, 287–338. [[CrossRef](#)]
33. Orikasa, H.; Tomita, A. A Study of the HCN Formation Mechanism during the Coal Char Gasification by O<sub>2</sub>. *Energy Fuels* **2003**, *17*, 1536–1540. [[CrossRef](#)]